Wilkinson[23] states that isotopic spin is not a very good quantum number in this region, the impurity ranging from 10 to 50% in intensity. Better data on all these reactions might permit a more accurate determination of the impurity.

An alternative explanation of the difference is that the $N^{14}(d,n)O^{15}$ reaction proceeds largely by means of a surface reaction, while the photonuclear reactions proceed mainly by compound nucleus formation. The angular distribution measured by Nonaka *et al.*[3] can be fitted reasonably well using the exchange stripping theory of Owen and Madansky[9] mentioned previously, as is shown in Fig. 8. If $N^{14}(d,n)O^{15}$ is predominantly a surface reaction, then it may be coincidental that some of the peaks in the yield curve correspond to energy levels found in the photonuclear reactions. The discussion on the $N^{15}(d,n)O^{16}$ reaction concerning stripping angular distributions and resonant yield curves can also be applied to this reaction.

[23] D. H. Wilkinson, Phil. Mag. **1**, 379 (1956).

ACKNOWLEDGMENTS

We wish to thank Dr. L. J. Lidofsky, Mr. T. H. Kruse, and Mr. J. A. Baicker for their assistance throughout the course of the experiment. The N^{15} was provided by Professor T. I. Taylor and Dr. W. Spindel, Department of Chemistry, Columbia University. We also wish to thank Professor G. E. Owen, Professor L. Madansky, and Dr. B. Margolis for discussion of the theory of these reactions.

PHYSICAL REVIEW VOLUME 112, NUMBER 6 DECEMBER 15, 1958

Elastic Scattering of C^{12} from Gold*

E. GOLDBERG AND H. L. REYNOLDS
Radiation Laboratory, University of California, Livermore, California
(Received August 18, 1958)

The angular distribution of C^{12} ions elastically scattered by gold has been measured at the following laboratory energies: 118±2, 101±2, 79.4±3, and 73.6±3 Mev. Heavy ions from the Berkeley heavy-ion linear accelerator (HILAC) were recorded in two Ilford E-1 plates from a scattering angle of 19° to 159°. In all cases the differential cross sections exhibited a Coulomb-like behavior at small angles, a rise above Coulomb of about twenty percent as the scattering angle increased, and then a rapid drop below Coulomb in much the same manner as alpha particles scattered from heavy elements in the 20–40 Mev range. The Blair "sharp cutoff" model reproduces closely the character of the data; however, small oscillations predicted from the model are not experimentally observed. Interaction distances of (11.8±0.3, 12.1±0.3, 11.85±0.4, and 11.85±0.45)$\times 10^{-13}$ cm, respectively, for the foregoing energies are inferred from application of the Blair model.

INTRODUCTION

FROM the time of Rutherford's classic experiment,[1] the elastic scattering of nuclear particles has been used in the study of the nucleus and nuclear forces. Recently the elastic scattering of α particles of intermediate energy (10–50 Mev) by nuclei has received considerable attention.[2–7] Analysis of this data by means of the Blair[8,9] "sharp cutoff" model and by the optical model[10,11] has been quite successful. The α-particle elastic scattering is particularly useful in the study of the nuclear potential at the edge of the nucleus since the mean free path of α particles in nuclear matter is small. The mean free path and the ability to penetrate barriers will be reduced as the size and charge of the elastically scattered particle increases, leading to the conclusion that the elastic scattering of particles heavier than α particles should provide useful information concerning the outer surface of the nucleus.

The first experiment involving the elastic scattering of energetic particles heavier than α particles was done by Reynolds and Zucker[12] and concerned the scattering of N^{14} by N^{14}. In spite of the added complexity introduced by the identical nature of the particles the "sharp cutoff" model showed good agreement with the results.

The heavy-ion linear accelerator (HILAC) at the University of California Radiation Laboratory produces an average beam current of 0.5 μa of heavy ions from carbon through neon with energies of 10.2 Mev per nucleon. The beam energy may be reduced below

* This work done under the auspices of the U. S. Atomic Energy Commission.
[1] E. Rutherford, Phil. Mag. **21**, 669 (1911).
[2] G. W. Farwell and H. E. Wegner, Phys. Rev. **95**, 1212 (1954).
[3] Wall, Rees, and Ford, Phys. Rev. **97**, 726 (1955).
[4] Wegner, Eisberg, and Igo, Phys. Rev. **99**, 825 (1955).
[5] R. E. Ellis and L. Schechter, Phys. Rev. **101**, 636 (1956).
[6] Kerlee, Blair, and Farwell, Phys. Rev. **107**, 1343 (1957).
[7] J. R. Rees and M. B. Sampson, Phys. Rev. **108**, 1289 (1957).
[8] J. S. Blair, Phys. Rev. **95**, 1218 (1954).
[9] J. S. Blair, Phys. Rev. **108**, 827 (1957).
[10] W. B. Cheston and A. E. Glassgold, Phys. Rev. **106**, 1215 (1957).
[11] G. Igo and R. M. Thaler, Phys. Rev. **106**, 126 (1957).
[12] H. L. Reynolds and A. Zucker, Phys. Rev. **102**, 1378 (1956).

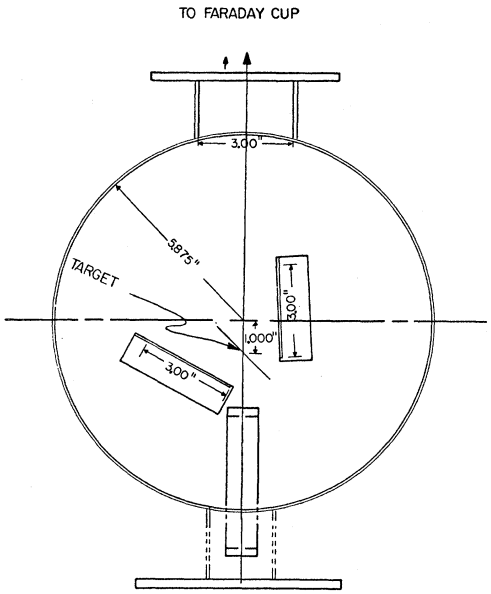

FIG. 1. Positions of emulsions in scattering chamber.

this peak value by appropriate use of absorbers. In this paper we discuss the elastic scattering of C^{12} from gold at laboratory energies of 118.3, 100.8, 79.4, and 73.6 Mev. At each of these energies the relative differential cross sections as a function of scattering angle have been obtained. The differential cross sections exhibit a similar behavior to those obtained with α particles. At sufficiently small angles the ratio of observed cross section to Coulomb cross section is unity. As the scattering angle increases, an increase in this ratio of about 20% is observed, after which a sharp drop occurs which apparently continues beyond the limits of our measurements.

The data have been analyzed in terms of the Blair "sharp cutoff" model.[8] The assumption in this model is that the amplitude of the outgoing lth wave is equal to zero if the corresponding classical distance of closest approach is equal to or less than the sum of the radii of the two nuclei. For l values larger than this critical l' the assumption is that the amplitude of the outgoing wave is that for pure Coulomb scattering. For the data considered, the critical l' values have been found to range from 29 to 65. The calculation reproduces the general character of the data. However, the rapid oscillations present in the calculation are not observed in the experiment. Values for the interaction distance have been inferred from the angular distributions.

EXPERIMENTAL PROCEDURE

A scattering chamber was constructed which allowed a collimated beam of ions to strike a thin gold target. The scattered particles were then deflected to nuclear emulsions while the main beam passed on to the collector cup. The chamber is shown in Fig. 1.

A group of interchangeable aluminum foils which served to degrade the ion energy preceded the scattering chamber. The collimator consisted of two $\frac{1}{16}$-in.$\times\frac{1}{2}$-in. slits separated by $7\frac{1}{2}$ in., and defined the beam which entered the scattering chamber. In initial studies considerable fogging of the emulsions occurred. This was reduced sufficiently by suitable placement of lead absorbers to remove x-rays and by the removal of the electrons from the beam. The latter was accomplished by straddling the beam with a permanent magnet directly in front of the collimator. The magnet caused a displacement of $\sim$14° for 2-Mev electrons but only $\sim$0.12° for 122-Mev C^{12} ions. This insured the removal of the electrons but left the C^{12} ions undisturbed. A thin aluminum foil (2.81 mg/cm^2) was mounted in front of the collimator to keep light out of the chamber.

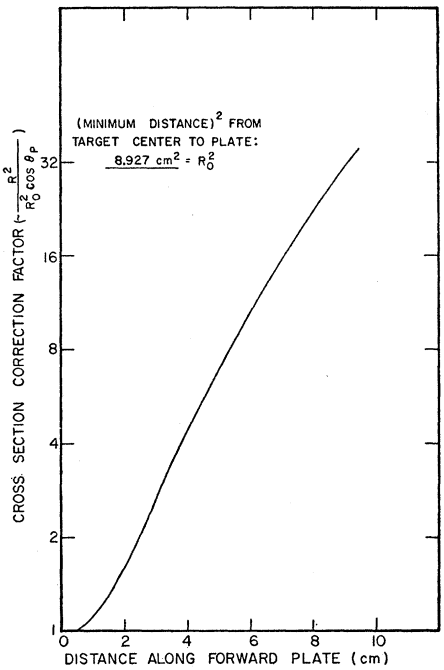

FIG. 2. Correction factor *vs* distance along forward plate.

The target was an unsupported gold foil, 0.75 mg/cm^2 thick. It was prepared by vacuum deposition upon a plastic foil. A ring holder was glued to the foil after which the plastic backing was stripped away. The target was oriented at an angle of 45° to the beam so that scattered particles to be detected would not strike the ring holder.

Ilford E-1 emulsions, 200 μ thick, acted as detectors. The plates were 1 in.$\times$3 in. and were placed in carefully machined plate holders. The edge of the plate nearest the target rested against a shoulder of the plate holder which insured accurate specification of the emulsion position with respect to target and beam axis. The emulsions, which were uncovered, were held in place with a thin film of Duco cement.

The angular range covered by the forward plate was 18.6° to 89.9°, while the rear plate covered 81.3° to 158.7°. The maximum particle range in emulsion was 190 μ so that the complete range of the particle was observed in the emulsion for all scattering angles. The C^{12} ions were identified by their heavy ionization, range, and angle of entry into the emulsion.

After passing through the target, the beam was collected in a Faraday cup and measured with a standard current integrator. No attempt was made to measure absolute cross sections. Two exposures were made at each energy, differing in integrated current by a factor of ten so that a large variation in scattering cross section could be detected with a reasonable number of tracks per unit area. The integrated charge for the heavier exposures was 1.4×10^{-5} coulomb which required about fifteen minutes of exposure indicating

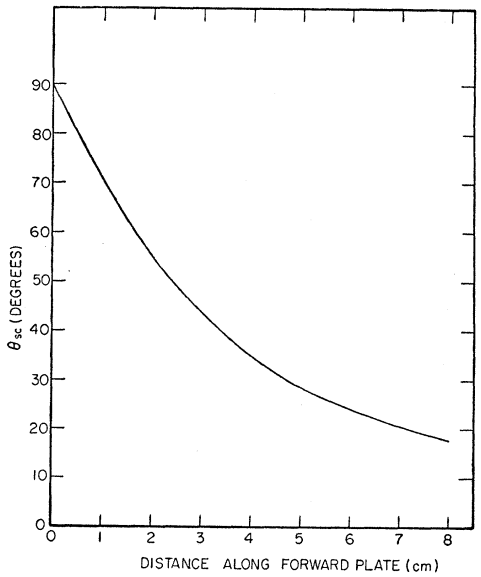

FIG. 3. Scattering angle from target in forward plate (lab system) *vs* distance along forward plate.

an average current of about 1.6×10^{-8} ampere through the collimating system. The drop in beam intensity from 0.5×10^{-6} ampere is due primarily to the collimator.

The number of tracks per unit area was determined with a standard Leitz binocular microscope and a Whipple disk. Approximately three hundred tracks were counted at each setting. The scattering angle was found from measurements of the geometry of the scattering chamber. The emulsion holders, target, and collimator were all mounted permanently on a single plate so that changes in geometry could not occur. The geometric correction factor for laboratory cross-section determination is shown in Fig. 2. This is simply related to the effective solid angle per unit plate area, as seen from the target. The scattering angle as a function of distance along the forward plate is shown in Fig. 3.

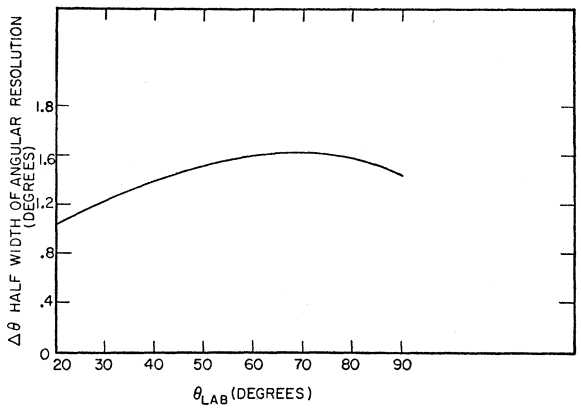

FIG. 4. Half-width of angular resolution *vs* scattering angle (upper limit).

The geometry of the scattering chamber was measured with calipers and micrometer to an accuracy of ±0.2 mm. The error in scattering angle due to the error in chamber geometry measurements was $\pm0.6°$, and may be compared to an error of $\pm0.5°$ which arose from chamber orientation with respect to the beam axis. However, the major contribution to the angular resolution is the finite width of the collimating slits. The angular resolution due to slit width is a strong function of the scattering angle not only because of the change in target-plate distance, but also the change in effective target size. The width of the beam on the target also changes with energy, because of the use of aluminum absorbers in front of the collimator. With no absorbers, the width of the beam on target is 1.6 mm, whereas multiple scattering in the absorbers can allow the collimator angle to be filled changing the above value to 2.3 mm. In a 5-mil aluminum foil, (the maximum thickness used in the present experiment) the rms angle of multiple scattering for 100-Mev particles is 1.4°. Multiple scattering in the target itself is not negligible. For 100-Mev ions, the half-width is about 0.6° and is a slight function of angle as well. The angular resolution due to finite collimator width and

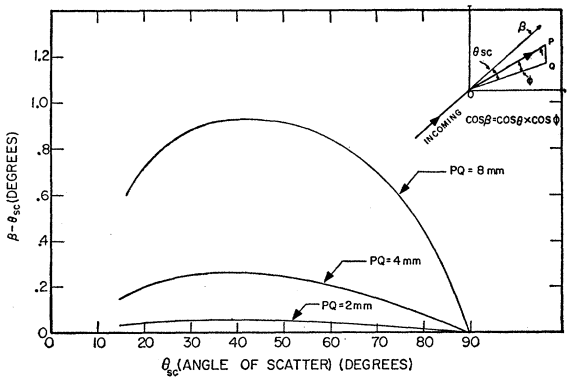

FIG. 5. Maximum error in swath length *vs* scattering angle for different swath half-lengths, i.e., *PQ* as shown in insert.

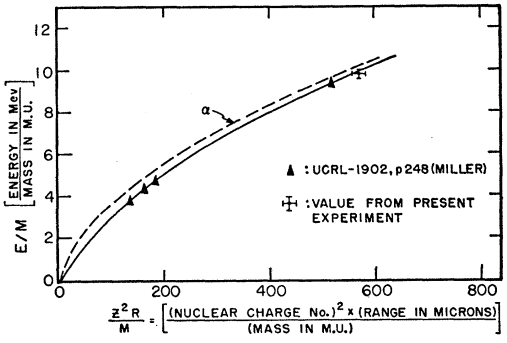

FIG. 6. Range-energy curve for C^{12} in Ilford E-1 emulsions.

multiple scattering in the foil is shown in Fig. 4. It has been pointed out by McIntyre[13] that a spread in beam energy is also reflected as a loss in angular resolution. This effect was evaluated by use of the sharp-cutoff model. It was found that a half-width in energy of 1.7 Mev leads to a half-width in angular resolution of 0.65 degrees at 120 Mev. At 70 Mev, this energy half-width is equivalent to a half-width in angular resolution of 3.4 degrees. Figure 4 does not include this contribution. Errors from chamber orientation and chamber geometry contribute fixed errors in angle.

If a large area of the emulsion is scanned so that the swath length is appreciable, an error in angle results

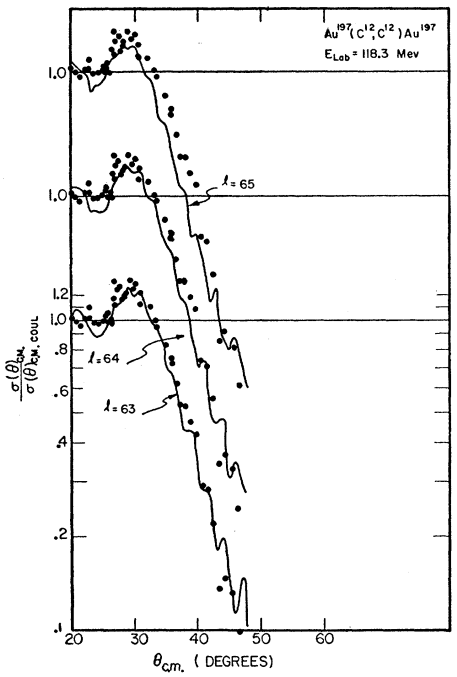

FIG. 7. Ratio of the differential cross section for elastic scattering of C^{12} by gold to Rutherford at $E_{lab}=118.3$ Mev. The ratio is normalized to unity at small angles. Experimental points are indicated by dots, and solid curves are those computed from the "sharp cutoff" model.

[13] J. A. McIntyre (private communication).

since the true scatter angle is not constant along a line in the plate normal to the base plane. The maximum change in angle as a function of scattering angle for various half-lengths of the swath (i.e., distance moved away from the plate center) is shown in Fig. 5. The distance in question was usually less than 3 mm resulting in a negligible error in angle. Corrections were made where the displacement was excessive. Note that the finite height of the collimator slits acts in a similar way. The true scattering angle exceeds the scattering angle of Fig. 3 by not more than 0.2° and is therefore neglected.

The initial energy of the beam is known to be 122±2 Mev from the length and radio-frequency of the accelerator.[14] Phase acceptance conditions are expected

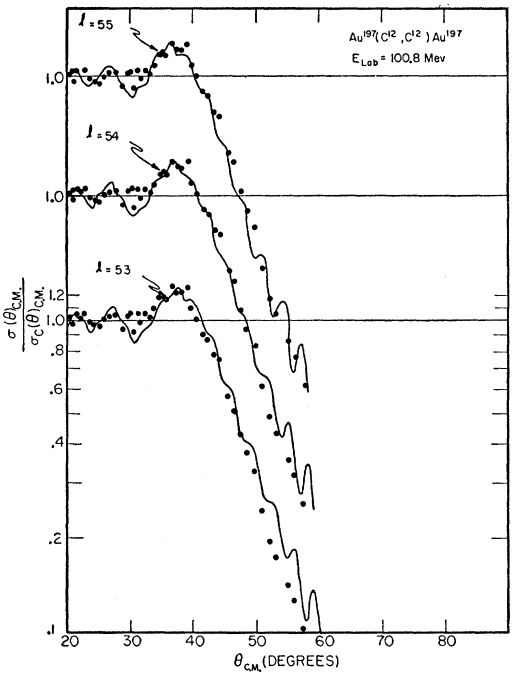

FIG. 8. Ratio of the differential cross section for elastic scattering of C^{12} by gold to Rutherford at $E_{lab}=100.8$ Mev.

to give rise to a beam energy spread of 3% full width; the peak of the energy distribution may vary by ±2 Mev from the calculated energy. The shifts could arise from such effects as nonuniform voltage gradients within the main HILAC tank. The energy of the beam can also be determined from the range of the scattered particles in the emulsion if the range-energy curve in emulsion is known. Miller[15] has given an experimentally determined range-energy curve of C^{12} ions in emulsion, which is shown in Fig. 6 together with the same curve for α particles. This can be checked for the upper energy point by comparison with the known energy of

[14] E. Hubbard (private communication).

[15] J. F. Miller, University of California Radiation Laboratory Report, UCRL-1902 (unpublished).

the beam from the accelerator. The measured range for the particles scattered at 20° for the maximum energy plate is also shown. Before reaching the plate the beam passed through 2.81 mg/cm² of aluminum and 0.94 mg/cm² of Au. The energy loss in these materials can be determined by multiplying the energy loss of equal-velocity α particles by nine since the carbon ions are completely stripped of electrons at these energies. The energy obtained for the beam was 124.2 Mev, indicating that Miller's range curve[15] is in disagreement by 2 Mev, or 1.7%. For the lower energy exposures this same percentage was used to correct the energy as obtained using Miller's curve. The exposure at the second to highest energy gave a HILAC energy of 125.4 Mev, knowing the aluminum absorber thickness and using

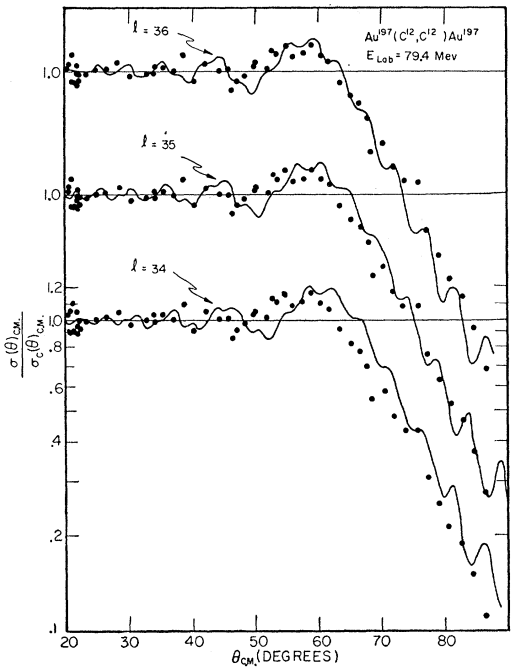

FIG. 9. Ratio of the differential cross section for elastic scattering of C^{12} by gold to Rutherford at $E_{lab}=79.4$ Mev.

Miller's curve; C^{12} energy loss was inferred from α-particle loss in aluminum since the C^{12} should be fully stripped. The lowest energy exposure gave a HILAC energy of 127 Mev, but since the latter number has the largest uncertainty it is not taken seriously. It is thought proper than an uncertainty of ±3 Mev should be assigned to the lowest energy exposure. Since the thickness of aluminum absorber was not registered for the second to lowest energy exposure, the energy is cited according to the recipe where comparison of range to Miller's curve is made. An uncertainty of ±3 Mev is also assigned to this exposure. The average energy loss in the gold foil was <1 Mev. It has been assumed in the determination of the energy of the carbon ions at the time of scattering that the scattering

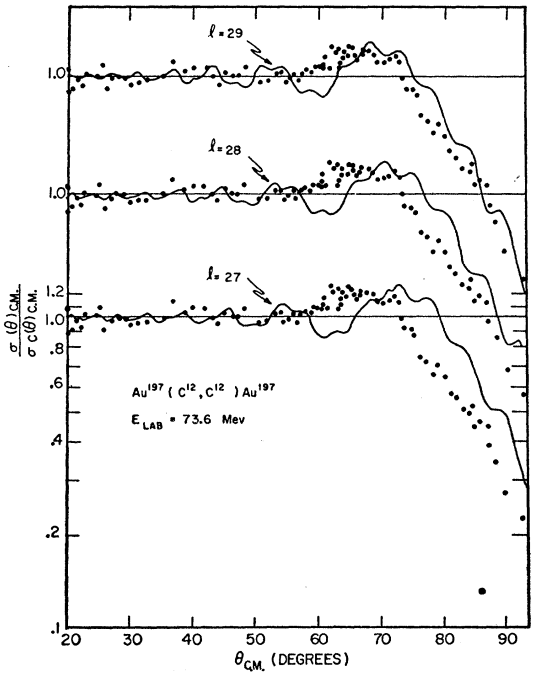

FIG. 10. Ratio of the differential cross section for elastic scattering of C^{12} by gold to Rutherford at $E_{lab}=73.6$ Mev.

took place when one-half of the foil had been penetrated by the beam.

RESULTS

The data are presented in Figs. 7, 8, 9, and 10 for laboratory energies of 118.3±2.0, 100.8±2.0, 79.4±3.0, and 73.6±3.0 Mev, respectively. The differential cross section in the center-of-mass system, $\sigma(\theta)$, divided by the Coulomb cross section in the center-of-mass system, $\sigma_C(\theta)$, is plotted *versus* the scattering angle in the center-of-mass system. For purposes of normalization, it has been assumed that the ratio fluctuates around unity at small angles. Each point represents 300 tracks giving a statistical standard deviation of approximately 6%. The curves shown are the results of calculation and will be discussed later. The errors in counting the tracks are less than 1% as shown by the comparison of counts for the same area, carried out by independent observers.

At all of the energies the measurements were carried out to angles where the cross section was approximately $\frac{1}{10}$ of the Coulomb cross section. At this point the problem of particle identification occurred. This is illustrated in Fig. 11 where a plot of the range spectrum is given at a laboratory angle of 48.9° for the 118.3-Mev plate where $\sigma(\theta)/\sigma_C(\theta)<0.1$. The spectrum is considerably broader than shown in Fig. 12, which is for a laboratory angle of 23.7°, indicating that inelastic events and fragmentation are very likely occurring at 48.9°. The broadening in the spectrum is not observable for this plate where $\sigma(\theta)/\sigma_C(\theta)\geqslant 0.2$. Although a careful selection of tracks could eliminate most of the inelastic

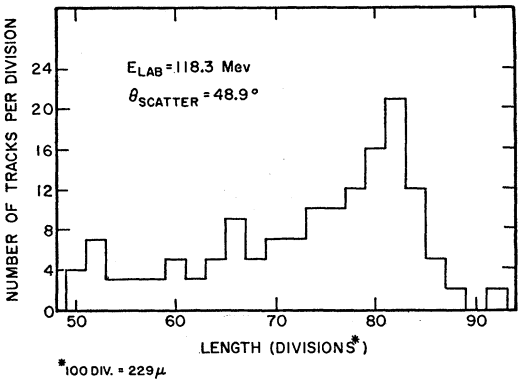

FIG. 11. Range spectrum of C^{12} tracks at $E_{lab}=118.3$ Mev and $\theta_{scatter}=48.9°$.

events, the removal of particles where A or Z has changed slightly would be very difficult. Accordingly efforts were not made to extend the measurements beyond the point where $\sigma(\theta)/\sigma_C(\theta)$ was 0.1. It is quite possible that inelastically scattered particles which have been degraded only one or two Mev are included as elastic particles. For example, when $E_{lab}=118.3$ Mev and $\theta_{sc}=23.7°$, the width of the energy spectrum was 2.7 Mev at half-maximum height.

Since routine current measurements were made it is possible to determine the absolute cross section to check the internal consistency of the measurements. It was found that the absolute cross sections in the Coulomb region were in agreement with the calculated values to within 30%.

For the lowest energy plate (73.6 Mev, Fig. 10) the region from 20° to 50° should have a zero slope of $\sigma(\theta)/\sigma_C(\theta)$ since it would not be expected that the nuclear potential would affect the cross section here other than to cause minor oscillations. However, in this region the value of $\sigma(\theta)/\sigma_C(\theta)$ changes by 5%. This would occur if the scattering angle was in reality 0.5° larger than determined from the geometrical measurements. Such an error is within the expected deviation in angle, and could be accounted for if the chamber axis were out of line with the beam axis to the extent of 0.5°.

DISCUSSION

The elastic scattering of α particles from heavy nuclei shows the same initial rise and subsequent sharp drop in $\sigma(\theta)/\sigma_C(\theta)$ with increase in scattering angle that is exhibited by the present C^{12} data in Figs. 7 through 10. As would be expected, the α-particle data is fitted to a high degree of precision by optical model calculations.[10,11] Of other attempts at analysis the most successful has been the "sharp cutoff" model of Blair.[8,9] Modifications of the Blair model by reducing the sharpness of the cutoff have not appreciably improved the agreement with the data.[3,5] In the Blair model the nucleus and scattered particle are considered spherical with definite radii. It is assumed that if the potential barrier of the lth wave allows the particles to overlap, the outgoing lth wave is destroyed. Analytically the amplitude for pure Coulomb scattering can be represented as a summation over l from zero to infinity of the amplitude for each of the outgoing l waves. Blair's model subtracts from this summation the contribution of the l values from zero up to the critical or cutoff l' value. The ratio of the cross section to the Coulomb cross section can be represented as

$$\frac{\sigma(\theta)}{\sigma_C(\theta)}=\left[\sin\mu^*+\frac{\mu'}{\eta^2}\sum_0^{l'}(2l+1)P_l(\cos\theta)\cos V_l\right]^2+\left[\cos\mu^*+\frac{\mu'}{\eta^2}\sum_0^{l'}(2l+1)P_l(\cos\theta)\sin V_l\right]^2,$$

where

$$\eta=zZe^2/\hbar v,$$

$$V_l=2\sum_{l''=1}^{l}\arctan(\eta/l''),\quad V_0=0,$$

$$\mu'=\eta\sin^2(\theta/2)$$

$$\mu^*=\eta\ln\sin^2(\theta/2).$$

Because of the simplicity of this model and its success in predicting the α-particle scattering results, it has been used to interpret the carbon scattering data. Since the cutoff l' value is 65 for the maximum energy measured the calculation was coded for the IBM 650 computer. A calculation at one-degree intervals from 20° to 120° with a cutoff l' value of 100 required approximately twenty minutes of computing time. Five adjacent cutoff l' values were treated simultaneously, and were centered around a specified l'.

Comparison of the "sharp cutoff" model with the optical model for α-particle scattering have been made

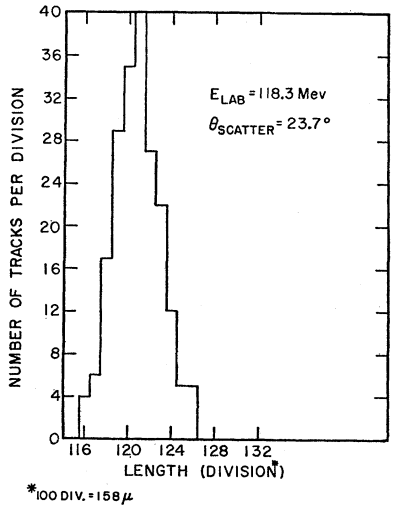

FIG. 12. Range spectrum of C^{12} tracks at $E_{lab}=118.3$ Mev and $\theta_{scatter}=23.7°$.

by Cheston and Glassgold[10] and Blair.[9] The former show with an optical model that the l value contributions to the reaction cross section in α-particle scattering decrease rapidly in the vicinity of Blair's critical l value. This substantiates the assumption of Blair that the nucleus absorbs all particles with orbital angular momentum less than the critical value l'. The applicability of the Blair model is determined by the sharpness of the cutoff. If the cutoff is to be sharp, there must be no leakage of particles through the barrier for l values greater than l' and no reflection of particles with l values less than l'. As stated by Blair,[9] the change from pure Coulomb scattering to complete absorption as l decreases will be more rapid for heavy ions than for α particles of the same velocity because of the decreased transmission and reflection of the barrier.

The calculations are shown together with the data in Figs. 7 through 10. The rise and sharp break are reproduced well. However, the oscillatory behavior is more extreme than that of the data. The calculated cross-section ratios for three adjacent cutoff l' values have been placed on each curve. The data have been reproduced for each of the curves.

The emulsions were carefully scanned in the regions preceding the rise, at the rise, and at the falloff. The dip preceding the rise which was predicted by the sharp cutoff model was not observed experimentally. Statistics of $\pm 3\%$ were realized in the exposures at 73.6 and 79.5 Mev in the regions where the dip before the rise was expected.

Calculations on the C^{12}-Au system at a few different energies using the sharp cutoff model were performed at large scattering angles (beyond those investigated in the experiments). They showed a levelling off and oscillation around the cross-section ratio value of about 0.03. Inasmuch as the experimental data did not cover cross-section ratios below 0.1, no judgment can be made in regard to these sharp cutoff predictions. In α-particle scattering experiments, it was clearly demonstrated that the cross-section ratio continued to drop with

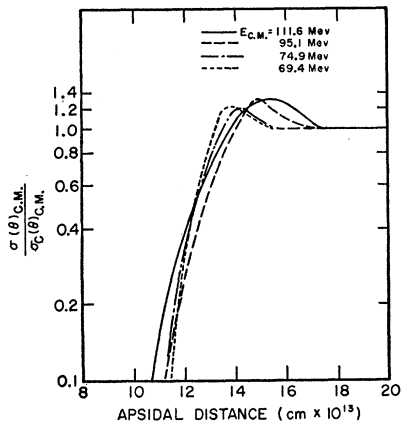

FIG. 13. Cross-section ratio as a function of apsidal distance at various energies.

TABLE I. Cutoff l' values and reaction cross sections.

$E_{c.m.}$ (Mev)	l'	σ_r (barns)
111.6±2	63±1.5	2.1
95.1±2	55±1	1.9
74.9±3	36±1	1.0
69.4±3	29±1	0.77

increase in scattering angle which contrasted with sharp cutoff calculations. The latter tended to oscillate around a value of 0.1.[4,9]

The experimental angular distributions of Figs. 7 to 10 have been transformed to cross-section ratios as a function of apsidal distance. The results are shown in Fig. 13. A good deal of similarity is noted among the four curves. Differences can be attributed to effects of interference among the partial waves. Alpha particles are seen to behave in a like manner.[4]

In trying to decide which cutoff l value gives the best fit to the data one must decide where the calculation, which is admittedly crude, should represent the data most accurately. The small oscillations in the calculation are due to the sharpness of the cutoff. Since the cutoff in nature will not be this sharp, it would be expected that these oscillations should be smoothed to some extent. It has been shown[10] that if one observes the amplitude of the real part of the lth partial wave as a function of l, it is oscillatory in sign as well as magnitude except in the neighborhood of the classical angular momentum l value, i.e., $l^*=\eta\cot(\theta/2)$. Here the amplitudes are all of positive sign. A similar behavior by the imaginary part of the lth partial wave is to be expected. The identity of signs of the partial waves in the region of l^* causes a sharp drop in cross section if these partial waves are removed; oscillations may be expected to persist even in the region of the sharp drop but should have a very minor effect on the position of the drop. It appears that the best region for fitting the calculation to the observations is in the region of the sharp drop in cross section.

Using this criterion, values of cutoff l' have been chosen and are listed in Table I. From the cutoff l value, l', the interaction distance, R, can be obtained from the equation:

$$E_{c.m.}=\frac{Z_1Z_2e^2}{R}+\frac{\hbar^2l'(l'+1)}{2\mu R^2}.$$

In Fig. 14 the cutoff l value as a function of center-of-mass energy has been plotted for several R values. The selected l values are shown at the four energies.

The interaction distances at laboratory energies of 73.6±3, 79.4±3, 100.8±2, and 118.3±2 Mev are (11.85±0.45, 11.85±0.4, 12.1±0.3, and 11.8±0.3) $\times 10^{-13}$ cm, respectively. The variation of the interaction distance with energy is within the probable error. In the case of α-particle scattering it has been noted that the interaction radius decreases with increasing radius.[9] If the relation $R_0=r_0(A_1^{\frac{1}{3}}+A_2^{\frac{1}{3}})$ is

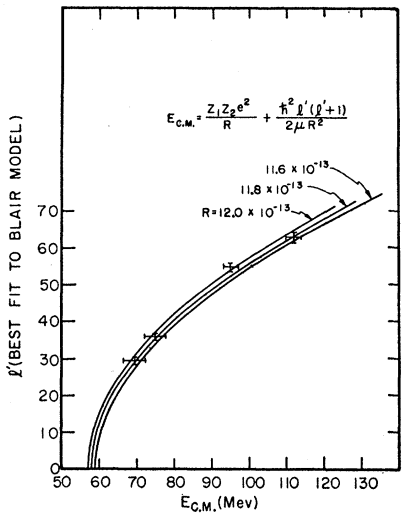

FIG. 14. Interaction distance for $C^{12}+Au^{197}$ at different c.m. energies inferred from "sharp cutoff" model.

employed, r_0 is 1.47×10^{-13} cm for an interaction distance of 11.9×10^{-13} cm. The uncertainties in R were determined from the dependence of R on E and l'. The latter quantity enters both explicitly and implicitly, for not only is there the uncertainty in the best choice of l' from the fits of data to theoretical curves, but also an error in E produces a set of l' curves based on this erroneous E. It was necessary to calculate the angular distributions according to the sharp cutoff model at an energy slightly displaced from the correct values to appraise the latter effect. The interaction cross sections have been computed using the relation

$$\sigma_r=\pi\lambda^2\sum_0^{l'}(2l+1),$$

and are given in column 3 of Table I.

The imaginary component of the nuclear potential, V_i, accounts for the absorption of the incident C^{12} particle. A crude but explicit expression which relates the mean free path of the C^{12} particle to this potential in the peripheral region is[16]

$$\frac{1}{\lambda^2}=\frac{4\mu}{\hbar^2}(E-V_{\text{coul}}-V_r)\left\{\left[\left(\frac{V_i}{E-V_{\text{coul}}-V_r}\right)^2+1\right]^{\frac{1}{2}}-1\right\}.$$

[16] Eisberg, Gugelot, and Porter, Brookhaven National Laboratory Report BNL-331, 1955 (unpublished).

If, in the peripheral region, the potentials are assumed to be $V_r\sim-20$ Mev, $V_i\sim-10$ Mev, and $V_{\text{coul}}\sim60$ Mev, the mean free paths are $\sim1.2\times10^{-13}$ cm at $E_{\text{c.m.}}=112$ Mev and $\sim0.8\times10^{-13}$ cm at $E_{\text{c.m.}}=69$ Mev. These values are smaller than those of α particles at corresponding velocities[11] because of the reduced mass, μ. One would expect, for such small mean free path values, that the interaction is almost completely determined by the tails of the nuclear potentials, V_r and V_i. The latter component is seen to be the much more important of the two. The variation of mean free path with energy would indicate an increase in interaction distance with a decrease in energy as observed with α particles.[9] However, the variation is very slight and it is entirely reasonable to expect that the correlation is masked in the present findings by experimental uncertainties. Data of higher accuracy and with better angular resolution would be of great value in determining the actual dependence of interaction distance on energy. Analysis of the present data by optical model procedures should clarify some of these questions. Such an analysis should establish further insight into the nature of the nuclear potential in the region of the nuclear surface.

ACKNOWLEDGMENTS

We are indebted to many persons who assisted in making this work possible. Dr. Edward Hubbard and Dr. Robert Main of the HILAC staff at Berkeley, California, assisted in making the exposures. Mr. Albert Oliver developed the emulsions. Mr. Bart Williams prepared the code for the IBM 650 computer. The targets were prepared by Mr. Dan O'Connell. We are especially indebted to Dr. T. C. Merkle for his support and encouragement.

Note added in proof. If relativistic effects are taken into account, the HILAC energy is found to be 124.5 Mev rather than 122 Mev. The quoted energies should therefore be increased by about two percent. The sharp cutoff calculations remain valid except for the fact that they apply to the new energy values. Interaction distances are found, as a result, to decrease by one percent from the quoted values, and are assigned at the new energy values.